1 **A New Way to Estimate Maximum Power from Wind Turbines: Linking**
2 **Newtonian with Action Mechanics**
3

4 Ivan R. Kennedy,[1,3,*] Migdat Hodzic,[2] Angus N. Crossan,[3] Nikolas Crossan,[3] Niranjan Acharige,[1]
5 John W. Runcie[1]
6
7 [1]School of Life and Environmental Sciences, Institute of Agriculture, University of Sydney, NSW
8 2006, Australia
9 [2]Faculty of Information Technologies, The Dzemal Bijedic University of Mostar, Mostar 880000
10 Bosnia and Herzegovina
11 [3]Quick Test Technologies, c/- Institute of Agriculture, University of Sydney, NSW 2006, Australia
12
13 Corresponding author: ivan.kennedy@sydney.edu.au
14

15 **Abstract**
16 A more accurate way to calculate power output from wind turbines based on fundamental Newtonian
17 mechanics is proposed for testing. This contrasts with current methods regarded as governed by flows
18 of kinetic energy through an area swept by rotating airfoils. Action mechanics measures torques caused
19 by conservation of momentum of impulsive air streams on rotor surfaces at differing radii. We integrate
20 the windward torque using inputs of rotor dimensions, the angle of incidence and strength of wind
21 impulses on the blade surfaces. A reverse torque in the plane of rotation is estimated as radial impulses
22 from the blade's rotation. Net torque is converted to power by the angular velocity of the turbine rotors.
23 A matter of concern is significant heat production by wind turbines, partly from leeward reactions but
24 mainly from turbulent release of vortical energy. Use of wind farms as sources of renewable energy
25 may need better practice, minimizing environmental impacts guided by this hypothesis.
26
27

28 ### 1. Introduction
29 Current models of wind turbine function use aerodynamic principles derived largely from airfoil and
30 propeller theories. The Rankine-Froude momentum and actuator disk models were developed in the
31 19th century with Betz and later Glauert (1935) providing refinements related to wind turbine
32 efficiency, including more recent developments (Sorensen, 2015). These models may include losses
33 from the axial motion of the air induced by rotors, in marked contrast to the radial action model
34 proposed here that assumes turbine blades generate power while rotating into undisturbed air,
35 independent of the down-wind wake.
36

37 A detailed explanation of the more recent blade element momentum theory (BEM) need not be given
38 here. In brief summary, BEM leads to an inexact expression for power output (P) according to the
39 following equations (1) and (2) as a function of the cube of wind velocity (v), air density (ρ), the area
40 swept (A_D) by the rotor blades with diameter D and a specific axial induction factor (a) related to
41 changes in angular momentum of the air flow.
42

43
$$P = [0.59v^3\rho A_D]/2 \tag{1}$$

2

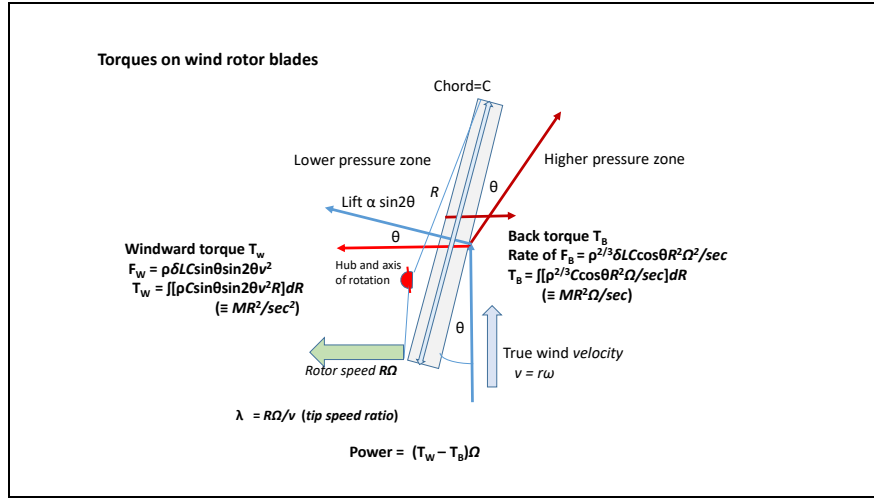$$P \ = \ 2a(1 - a)^2 v^3 \rho A_D \qquad\qquad (2)$$

This enables power extraction for a system that includes a rotating wake, claimed to give a maximum power consistent with the Betz limit for power from the kinetic energy of 0.593. Taken with other inefficiencies, a power output of about 30% of the theoretical maximum possible from kinetic energy is found in practice. Forces from air flow over an airfoil responding to angular dimensions of the blade are decomposed into lift and drag, normal and tangential to the apparent wind speed. This enables estimates of forces rotating the turbine and those just bending the rotor to be separated, taking the axial factor (a) of equation (2) into account to estimate torques. However, we will point to flaws in this model, caused by mismatching the interception of wind energy by the blades and the use of a model of the inertial power of wind we judged as inferior (Kennedy and Hodzic, 2021a).

We have defined with action mechanics statistical variation in radial separation and temperature of molecules undergoing impulsive collisions, allowing estimation with the accuracy needed to calculate the action and entropy of atmospheric gases (Kennedy et al., 2019). In our subsequent revision of the Carnot cycle (Kennedy and Hodzic, 2021a, 2021b), such molecular action states were found to define the density of quanta that establishes a Gibbs field needed to sustain the molecular kinetic pressure responsible for work processes. Molecular kinetic energy alone was insufficient to explain these processes. This complementary notion of the significance of the Gibbs action field challenges the widespread assumption that heat is merely molecules in motion.

We speculated during 2021 that similar complementary action processes might explain the inertial wind pressures acting on the blades of turbines. The scientific question we ask is whether this developing theory can be a more accurate way to estimate power output from wind turbines by using a similar coupling of Newtonian to action mechanics (Kennedy et al., 2021). Given Isaac Newton's youthful interest in the causal theory of windmills shown by his recently discovered inscriptions on the farmhouse walls at Woolsthorpe, this possibility seems apt. The purpose of this paper is to test this hypothesis from its predictions, allowing the exercise of Ockham's razor to judge its success.

1.1 *Radial action theory*

In the radial-action model for estimating wind power the details of blade aerodynamics need only be considered later as refinements. Similar to Carnot's purpose in defining cycle for heat engines (Kennedy and Hodzic, 2021a) the radial action cycle for wind turbines should be considered as an ideal estimate of the maximum possible motive power. Inefficiencies from friction or other causes will not be dealt here. Radial action mechanics should apply to rotor blades of any shape, while the fundamental differences in geometry and the torques generated by the windward [T_w] and leeward surface [T_b] must be respected. Figure 1 models the torques generated on the blade surface areas, allowing the maximum power to be estimated as a function of windspeed, its angle of incidence and the actions and reactions in the blade surface material, controlled by the blade length (L or R). chord width (C) and the tip-speed ratio [$L\Omega/v = \lambda$] of rotor tip speed [$L\Omega$] compared to wind speed [v].

Figure 1. Windward (T_w) and leeward (T_b) back torques developed on a rectangular rotor blade. Equations were generated from trials using a numerical program using dimensions shown. The theory provides a theoretical maximum of power for a given angle of wind incidence, obtained by the difference between torques T_w and T_b, occurring at about θ=60°. Note the different dimensions employed for the density factor, explained in the text.
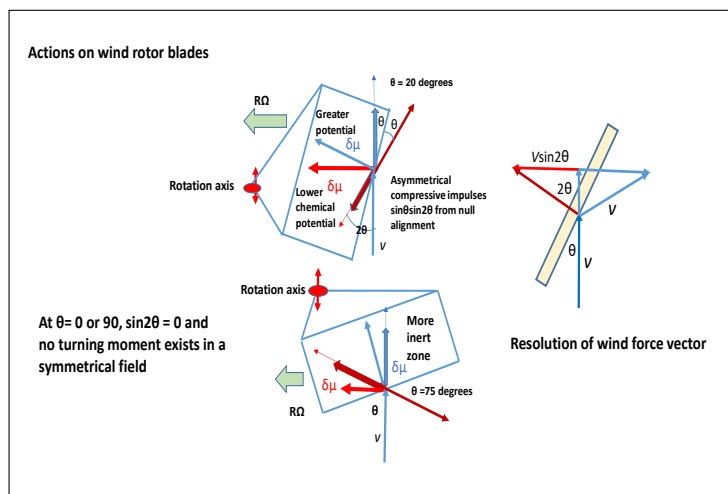
The main results found from our analysis of the impulsive action on the windward surface of the blade (Figs. 1, 2) follow.

(i)   Impulses [$δmv=δmrω$] generated by material particles on elastic rotor surfaces as envisaged by Newton's second law experimental approach to conservation of momentum power the turbine's rotation at the hub, if free to do so. The air particles impact on trajectories imposing the inertia of the wind velocity on their far greater microscopic velocities, with mean free paths of the order of picometers. Action impulses [$δmvR$, J.sec] with R the radial dimension to the hub, reflect the momentum of air trajectories from the surface. No detailed consideration needs to be given to the individual trajectories of the air molecules comprising wind, given that the transfer of momentum is collective. The rate of impulsive action [$T_w = ΣδmvR/δt$, J or N.m] provides the magnitude of the windward torque exerted.

(ii)   The angle of incidence θ is also the angle of reflection from a flat surface (Fig. 1), giving a total deviation angle of 2θ for the momentum. The decreased forward velocity is the source of effective lift normal to the flat surface, determined by this angular deviation.

(iii) A turning moment is exerted within the blade material in the plane of freedom of rotation of the turbine, at an angle normal to the direction of wind incidence. The magnitude of the turning moment [$Mv\sin2θ$] and its cause is illustrated in Figure 2.

(iv)   This application of Newton's second law requires that the true wind direction be considered to estimate the reaction on the turbine blade. The apparent change of wind direction caused by the rotation of the rotors, critical in BEM theory, is irrelevant in the radial action model. The current blade momentum theory using aerofoil theory as an analogue assumes lift normal to the blade and drag in the same direction as the blade; taking account of axial air motion downwind is an unnecessary confusion of cause and effect for impulsive radial action.

4

118   (v)   Two kinds of impulsive force on the blades need to be considered. The first is uniform with
119   length along the blade from reflected windward impulses on the blades' surfaces, giving
120   the torque generating the rotation; the second is a reaction torque also variable with blade
121   radius R from impacts by the rear of the advancing blades on air molecules, tangential to
122   the direction of rotation (Fig. 1). At tip-speed ratios greater than one, the back torque
123   involves impulses of greater magnitude than ever seen in airfoils unless rapidly gaining
124   altitude. As a result for most of the blade, except that adjacent to the hub, no drag force
125   operating in the wind direction can be caused by turbulence on the downwind surface given
126   the normal reaction from air molecules to the rear of the blade as Newton's marbles; drag
127   has little or no analogue in wind turbines (Figs. 1, 2). If the aerofoils of aircraft are
128   considered the same as the blades of wind turbines, the aircraft should be rotating around
129   its longitudinal axis as it is impelled forward by propellers or the thrust of jets. It is
130   suggested this discrepancy could make BEM theory a flawed approach.
131

132
133   **Figure 2.** Generation of turning impulse ($V\sin2\theta$) from the surface normal to the wind direction is shown for
134   two angles of incidence. Highly elastic action causes stresses and strain in reaction that intensify chemical
135   potential in rotor material, eased by rotation action exerted as a degree of freedom. For the perfect elasticity of
136   1.0, the turning moment imparted to the rotor balances that of the reflected momentum in the opposite direction.
137
138

139   **1.2 *Analyzing of the rotor-turning moment from wind pressure***
140   Whatever paths the individual air molecules take in flow near the blade surface, dictated as laminar
141   while the Reynolds number remains small, it is a fundamental principle of Newtonian mechanics that
142   the linear momentum at a given radial action is conserved. By Newton's experimental law the impact
143   of elastic bodies for oblique collisions on smooth surfaces will be reflected by the same angle for
144   coefficients of restitution of 1.0. However, part of the moment exerted by wind particles may be
145   extinguished if absorbed as thrust acting to push the wind tower and blades in a direction unable to
146   rotate the rotor on its axis. For smooth surfaces there is no force parallel to the surface and the
147   component of the particle velocity in the direction of motion is shown in Figures 1 and 2 as fully
148   conserved with the angle of reflection equal to the angle of incidence.

5

150 For oblique impacts in the range 0-90 degrees, asymmetric compression of blade material at the surface
151 are generated as an oscillating function, dependent on the elasticity and density of the blade material.
152 If the blade surface remains clean and elastic, this variation in stress as reactive pressure produces
153 strains distorting the windward surface, varying the chemical potential in the compressed zones as a
154 function of the angular deviation of the reactions. As a relationship between elastic stress and strain,
155 this reaction can be described as a function of Young's modulus (E) for the rotor surface material, with
156 surface stress σ or uniaxial force ($m\omega^2$) and strain ε equal to the distortion $\delta l/l$.

$$E = \sigma/\varepsilon \qquad (3)$$

160 For the blade material distal to the point of wind reflection, the physical reaction to the radial impulses
161 is distributed in an arc of (90+θ) degrees while for the proximal reaction the arc for compression is
162 (90-θ). The arc difference being 2θ, the turning moment per molecule on the rotor's axis is proposed
163 to vary with $mv\sin2\theta$, thus balancing action and reaction. At 90 degrees or $\pi/2$ radians, this function
164 becomes zero with any turning moment now symmetrical totally devoted to bending rather than turning
165 the blade on its rotational axis at the hub. Obviously, this analysis can only be applied to compressions
166 on the windward side of the rotor blades. The other factors determining the windward torque are the
167 density of air (ρ), the chord width (C) and $\sin\theta$, determining the volume and the mass of air impacting
168 the blade per second. This represents the instantaneous magnitude of mass impacting per second for
169 the area normal to the wind flux. When integrated with respect to the radius (R) over the entire length
170 of the blade (L) the cumulative torque [T_w] exerted at the hub is given in equation (4).

172 $$Tw \;=\; \int_0^L [\rho\delta LC\sin\theta\sin2\theta \, v^2 R]dR = \int_0^L [M\sin2\theta \, vR/sec]dR \quad [\mathrm{ML^2T^{-2}},\, \text{J or N.m}] \qquad (4)$$

174 This equation comprises factors for the 3-dimensional density of air (ρ), the area of the blade at R
175 ($\delta LC\sin\theta$), the momentum per sec [$\rho\delta LC\sin\theta v = Mv$] made normal to the wind by $\sin\theta$, the extent of
176 lateral reaction, thus [$Mv\sin2\theta$]. Numerically, the square of the wind velocity (v^2) is involved, once to
177 estimate the mass of air impacting the blade per second and second to establish the magnitude of action
178 impulse per second proportional to the variation in action (δmvR) per molecule. This is considered as
179 involving a rectangular blade in Figure 1 but different versions of the blade area at any radius can be
180 estimated from variations in the chord width (C) as a function of the radius to the hub (R). The 3-
181 dimensional density is regarded as a thermodynamic function, given that wind is a cooperative action
182 with its radial inertia involving not just the kinetic energy of molecules striking the rotors on the
183 windward surface, but with vortical energy and its resulting chemical potential. This vortical energy
184 unique to vortexes is explained in Results and in Discussion.

1.3 *Leeward torque of rotor blades*

189 It is said that a youthful Newton while designing his flour windmill estimated wind force by the
190 difference between the distances he could leap with and against the wind. This image is consistent with
191 our model of the impact of the inertia of the blade on that of air. In contrast to the windward torque

6

192 $[T_w]$ proportional to radius, in which the wind factor v^2 applies uniformly with radius R over the rotor
193 blade from hub to tip, the back torque (T_b) varies with the square of the radius, caused by the variable
194 rate of impacts on the air behind the blade variable with R during rotation. This variation is illustrated
195 in Figure 2. Given that the speed of rotation [$R\Omega$, m sec^{-1}] determines both the instantaneous mass of
196 air impacted per second as well at the radial momentum of these impacts, the specific action integral
197 required is of radius squared [$R^2\Omega$]. An initial run of the model using $R^2\Omega^2$ as a factor was found to
198 produce a function of power rather than torque. This justified integrating the specific action per radian
199 ($R^2\Omega$) instead of the energy per unit mass [$R^2\Omega^2$]. In effect, a variable inertial force along the blade is
200 integrated with respect to velocity to provide the correct rate of impact with mass.

202 An important difference between windward and leeward impulses with air molecules lies in the
203 irreversible nature of impacts from the blade on air molecules. While windward impulses may be
204 considered as a balancing of forces from the wind on the blade reaction, the leeward impacts generally
205 exceed the wind speed except near the hub and cooperative resistance from air at the rear of the blade
206 is much diminished and is ignored. As a result, the density of air molecules is effectively exerted from
207 2-dimensional action impulses exerted as a series of minute slices of air, varying with radius. If the
208 number density of molecules in a cubic meter is taken as proportional to n^3 then n^2 must represent the
209 density of molecules the blade encounters as a continuous process. Taking the density as having a
210 fractional exponent, the factor required should be $\rho^{2/3}$ or 1.145 rather than 1.225. By such a choice the
211 correct physical dimensions to describe the rate of transfer of momentum from the blade to air
212 molecules, integrated with respect to R, obtains the rate of impulsive action or reactive torque. The
213 inertial matter (MR) impacted per second expresses the action function $MR^2\Omega$ rather than momentum
214 $MR\Omega$, with decreasing orthogonality of impulses on shorter radii. To obtain the reverse torque,
215 equation (5) must be integrated

217 $T_b = \int[\rho^{2/3} C cos\theta R^2 \Omega/ \sec]dR = \int[MR^2\Omega/\sec]dR$ [ML^{2}T^{-2}, Nm](kg.m^2 per sec^2)   (5)

219 The surface area swept aside by the blade for each 1 meter segment of the length L is $C\cos\theta$, given
220 that the radius is varied to estimate torque for each decrease in the length of the blade. So the
221 momentum generated in each second at each radius is equal to the volume swept aside per
222 second [$C\cos\theta R\Omega$ x density ρ/sec = $MR\Omega$/sec]. Expressed as an action impulse depending on the
223 radius, that gives action per sec or torque [$\rho C Cos\theta R^2\Omega$/sec] or [$MR^2\Omega$/sec, ML^{2}T^{-2}]. The longer the
224 radius, the more orthogonal the impulse and the effectiveness of the action impact [mrv, J.sec].

226 Subtracted from the windward torque exerted on the front of the rotor blade to obtain the net torque
227 on the rotor, then multiplied by the number of blades and by the angular frequency Ω, the net power P
228 can be obtained. Both torque equations can be derived with a constant value for any configuration of
229 rotor operation and then integrated in a standard formula for R and R^2 respectively [integrals of $L^2/2$
230 and $L^3/3$] for accurate outputs, assuming ideal conditions. Taking the derivative of factors such as
231 angle of incidence, tip-speed ratio (λ) and rotor length (L) with respect to power allows optimization
232 of each of these factors. This should allow ease of control of these factors in wind turbine operation.
233 Optimum tip speed ratios are usually in the range of 3 to 10 with optimum length a function of wind
234 speed. Then turbine power (P) can be estimated by the difference of windward and leeward torques
235 multiplied by the angular frequency (Ω) of rotation.

236

237
$$P = [T_\mathrm{w} \ - \ T_\mathrm{b}]\Omega \qquad [\mathrm{ML^2T^3} \ \mathrm{J/sec}] \qquad (6)$$

238

239 Consistent with this introduction, a computer program described in Methods and Supplementary Text
240 was used to develop the theory, giving results consistent with equations (4 -6) described in the
241 following section.

242

243

244 **2. Results**

245

246 **2.1** *Power estimates for simulated commercial wind turbines*
247 Using available data on blade lengths and estimated chords a set of power outputs, assuming a
248 triangular blade without twist with an angle of wind incidence (θ) 55° and tip speed ratio (λ) as given
249 in Table 1. No attempt has been made in these estimates to optimize aerodynamics, with the windward
250 and leeward surfaces considered as flat and fully elastic. However, it is anticipated that attention to the
251 aerodynamics would produce some marginal effects on power output.

252

253 **Table 1. Power outputs from simulated commercial wind turbines**

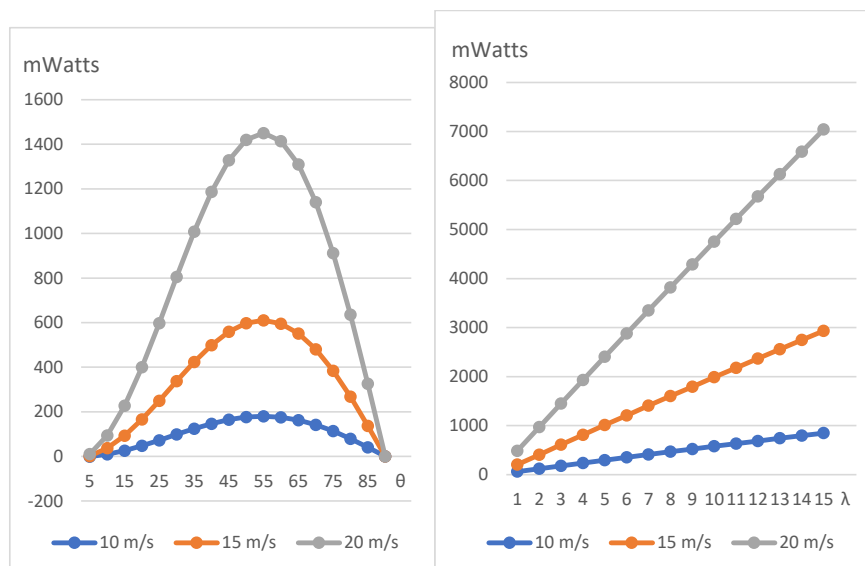| Brand	TSR (λ) $L\Omega/V_\mathrm{w}$	Wind m/sec	Chord C meters	Wind torque (Tw) MNm	Back torque (Tb) MNm	Power MW
Vevor 400	3	15	0.112	0.0000071229	0.00000006913	0.0006104
GE 1.5MW	8	15	3.025	0.61191	0.11339	1.54380
Nordex N60	8	15	3.250	0.41318	0.07557	1.35043
Nordex N131	9	15	3.500	3.46481	0.76443	4.55715
GE Haliade-X	10	15	8.000	11.41320	2.72240	13.0362
				Length (m)	Chord width (m)	Blade area (m²)
Vevor 500 mW				0.520+0.10 hub	0.023 -0.115	0.105
GE 1.5MW				38.75 +	0.10-3.025	183.0
Nordex N60				30 +1.0	0.25-3.25	120.0
Nordex N131	3900			63+2.5	0.25-5.0	487.5
GE Haliade-X	12 MW			100+ 8.5 stalk	0.5-8.00	1290.0

254 θ = 55°

255

256 Only in the case of the Vevor and Nordex N60 was performance data available to the authors, with
257 0.400 kW at 12 m per sec wind speed and 1.13 MW at 15 m per sec being claimed. Of several large
258 turbines examined, the Nordex claims were found to be the most modest with claims of 1.3 and 3.9
259 MW available in advertising material; several of the larger turbines about to be commissioned for
260 marine settings seemed too optimistic, particularly when the rating was conducted as sometimes
261 claimed with wind speed close to 10 meters per sec. We suggest that advertised successful field trials
262 over 24 hours may have been conducted with wind speeds greater than the rating speed.

263

264 A requirement for the radial action model was that it should be fully scalable with size. Figure 3 shows
265 power results calculated for a wind turbine fitted with 52 cm blades, equal to those of the Vevor
266 commercial model we purchased. Vevor claim power output of the order shown (Supplementary Text).

WIND
ENERGY
SCIENCE
DISCUSSIONS

eawe
european academy of wind energy

8

267   These results were obtained for triangular blades of average chord width of 6.50 cm, tapering from
268   2.30 cm at the tip 62.0 cm from the hub to 11.50 cm at the base, supported on a 10 cm stalk to the hub.
269

270
271   **Figure 3.** Radial action power output in milli-watts estimated for the Vevor 52 cm turbine showing optima for
272   55-60° wind incidence θ and increasing power with tip-speed ratio λ at all wind speeds. Data for torques Tw and
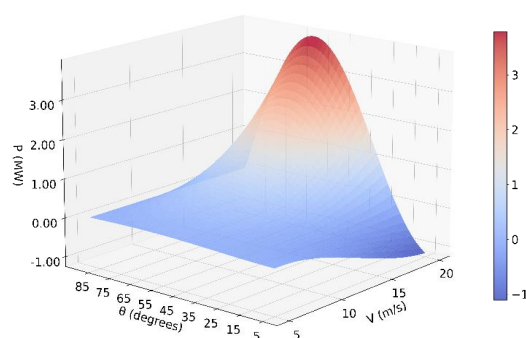273   Tb are given in Table S1 and S2 in Supplementary Text.
274
275
276   Unlike the larger GE 1.5MW and Haliade-X 12MW turbines , the back torque (T_b) was negligible
277   Table 1, reflecting the shorter radius and the R^2 factor involved. For the Vevor turbine the theoretical
278   tip speed ratio (λ) shown in Figure 3 above 4 is excessive, exceeding the limit of 800 rpm by the
279   manufacturer's guarantee. The program advanced chord width by 0.1769 cm for each iteration. When
280   data for the Vevor turbine were employed for a rating wind speed of 12 meters per sec with λ of 3.5, a
281   power output of 406 Watts was calculated. This result is in good agreement with the published rating
282   of 400 Watts. This result is consistent with accuracy of the radial action model, but it should be
283   experimentally tested such as in wind tunnels.
284

285   **2.2 *Estimates of predicted power output varying wind speed and tip-speed ratio***
286   Some representative results included in Supplementary Text using the radial action model varying
287   wind speed and tip-speed ratio similar to those expected for a General Electric 1.5MW wind turbine
288   of 83 m diameter are given in Figure 4. The data show how the windward [T_w] and leeward [T_b] torques
289   differ in character. The former shows a peak close to 55° diminishing towards 0° and 90°. By contrast,
290   the leeward torque is maximal near zero degrees angle [θ] of incidence, decreasing slowly with the
291   true angle of incidence to zero at 90°. Assuming a constant angular velocity, the potential power output
292   shown in the figure has a similar form to the windward torque. The curves assume a given tip-speed
293   ratio λ and rotational velocity. However, where there is no net torque (T_w-T_b) the rotor will not
294   commence or will stall at that angle of incidence. At a wind speed of 10 m per sec, the optimum value

9

295 of λ was 8, but when wind speed is 20 m per sec, the optimum ratio was even greater than 20, a value
296 challenging to the strength of materials, since the tip speed would then be 400 meters per second,
297 nearing the speed of sound in air.

298
299
300 **Figure 4.** Power simulation of 1.5MW turbine using the Wind turbine program A tip speed ratio of 8
301 was used for four wind speeds of 5, 10 15 and 20 m/sec used for the power diagrams, varying the
302 angle of wind incidence θ (lower panel). Data for varying tip-speed ratios are given in
303 Supplementary Text Figure S3.
304
305 **2.3 *Comparing kinetic and vortical energies in wind***
306 From action mechanics we have proposed (Kennedy and Hodzic, 2021a, 2021b) that air in anticyclones
307 and cyclones, subject to the inertial Coriolis effect, possesses a higher degree of freedom of action
308 superior to the accepted vibrational, rotational and translational degrees of freedom. This increased
309 source of entropy can be estimated from its vortical action, capable of magnifying the heat capacity of
310 air, depending on the radius of action and the vortical frequency or wind speed ($v=R\omega$). By comparison,
311 the kinetic energy of vortical motion has only a small fraction of the same energy capacity. This is a
312 testable hypothesis since it predicts that detectable thermal energy will be released as radiant heat from
313 the cascade of turbulent conditions. Furthermore, colliding air masses must also generate radiant heat
314 as laminar flow is replaced by turbulence. We consider it is normal function of anticyclones that they
315 should release radiant heat by friction with the surface (Kennedy and Hodzic, 2021a), an important
316 natural process transferring heat from the Hadley circulation of tropical air towards the poles. Too
317 much interference with such natural energy flows could lead to intrusion of colder polar air; this may
318 already be occurring in the polar vortices being experienced in both hemispheres.

10

319
320 We had originally assumed from our analysis of the Gibbs field in the Carnot cycle that vortical
321 entropic energy filling a higher degree of freedom of vortical action in anticyclones and cyclones could
322 be obtained using ambient temperature T expressed as Kelvin. For 3-dimensional translation of
323 molecules like argon or nitrogen mv^2 is equal to $3kT$. For a 3-dimensional velocity v, the temperature
324 (T) must equal $mv^2/3k$, where the translational velocity (v) is 3-dimensional for each gas molecule. By
325 contrast taking a 1-dimensional velocity ($v = r\omega$) as in horizontal wind in an anticyclone, we conclude
326 the equivalent temperature (τ) must equal mv^2/k where v is wind speed. With the assumption that
327 temperature is a statistical version of torque as given in our action revision of the Carnot cycle, the
328 calculation of mean value negative Gibbs energy must involve the following formula, replacing
329 ambient temperature T for air molecules with τ specific to the Gibbs field of wind velocity. Then for
330 an air molecule with wind velocity of v, the virtual wind temperature (τ) must equal mv^2/k.

331
332 $$-g_{vor} = mv^2\ln[n_{vor}] = s_{vor}\tau \qquad (7)$$

333
334 Table 2 provides details of data for vortical entropic energy for a cubic meter of air as wind 1000 km
335 from the center of an anticyclone. The greater magnitude of the vortical component indicates that wind
336 power is not so primary function of kinetic energy but more of the vortical energy of the Gibbs field
337 exerting torques, supporting the motion of the molecules. Calculation of vortical action ($@_{vor}$) and
338 entropic energy is shown in equation (15), where R is the radial distance to the center of the cyclonic
339 structure and $R\omega$ the steady windspeed at R from the center.

340
341 $$@_{vor} = mR^2\omega; \quad mR^2\omega/\hbar = n_{vor}; \quad \text{Vortical energy per molecule} = mv^2\ln[n_{vor}] \qquad (8)$$

342
343
344 **Table 2. Vortical energy properties for GE 1.5 MW wind turbine**

Wind speed ($m\ sec^{-1}$)	Vortical action ($@_v$)/molecule [J.sec, $\times10^{19}$]	Quantum number n_{vor} $\times10^{-15}$	1-D torque mv^2/molecule $\times10^{24}$	Vortical energy /molecule [$(mv^2)\ln(n_{vor})$, $\times10^{23}$ J]	Vortical energy [J/m³]	Kinetic energy [J/m³]	Ratio
5.0	2.4215	2.29615	1.2108	4.2826	1083.251	15.313	70.741
10.0	4.8430	4.59230	4.8430	17.4654	4417.740	61.250	72.126
15.0	7.2645	6.88845	10.8968	39.7391	10051.703	137.813	72.937
20.0	9.6860	9.18975	19.372	71.2054	18010.864	245.000	73.514

345 Radius = 1000 km

346
347
348 The relative vortical action and quantum state (n_{vor}) are proportional to wind speed but the vortical
349 energy and quantum field pressure (field energy/unit volume) are logarithmic functions of the action
350 as quantum numbers. The mean quantum size is exceedingly small and decreases with wind speed,
351 most of the work or quantum pressure driving the motion of anticyclones (or cyclones) being acquired
352 at lower temperature and wind speed. Given that air at 288.15 K and 1 atm pressure contains
353 2.5294×10^{25} molecules of air per cubic meter, the vortical field energy of air is 10.052 kJ per cubic
354 meter at a wind speed of 15 meters per sec (Table 2). For this calculation we assumed a mean mass of
355 29 Daltons for air molecules to estimate action.

11

356
357   For comparison, Table 3 gives results for associated wind kinetic energy with various wind speeds,
358   showing data corrected for the Betz limit of 0.593 for the maximum power said to be extractable.
359   Compared to the rate of kinetic energy passing into the area swept by the blades, the radial action
360   prediction of power is always less, so if a mechanism to harvest were available, this would be
361   sufficient. However, when the kinetic energy in the wind actually impacting on the blades is estimated,
362   this is insufficient to explain the predicted power output. By contrast, when the vortical entropic energy
363   is estimated (Kennedy et al., 2021) impacting the blades is compared, this is greater than either kinetic
364   energy and exceeds the actual power output estimated by about six times, almost an order of magnitude
365   greater.

366
367
368   **Table 3. Kinetic and vortical energy impacting a wind turbine similar to GE 1.5MW**

Wind speed (m/sec)	Kinetic energy per sec 83 m diam. (Betz) (J)	Kinetic energy /blade-area/sec blades	Vortical pressure (J/m^3) (blade area x v)	Vortical power (Watts, J/sec) estimated for blade area	Power estimated by radial action model (Watts)
					At λ=9, θ=55°
5.0	2.1670x10^5	8.4066x10^3	0.361069x103	0.33038x10^6	0.031168x10^6
10.0	1.7336x10^6	6.7253x10^4	1.47258x10^3	2.69482x10^6	0.40541x10^6
15.0	5.8509x10^6	2.2698x10^5	3.35055x10^3	9.19727x10^6	1.54381x10^6
20.0	1.3869x10^7	5.3802x10^5	6.00353x10^3	21.9729x10^6	3.86798x10^6

369
370
371   It is predicted that some of the even larger turbines planned for ocean platforms may not achieve the
372   performance anticipated. Given that the back torque is a function of the third power of the blade length
373   when integrated, whereas the windward torque is a function of the blade length squared, a decrease in
374   performance with increasing blade length is expected. These values were all calculated with chord
375   length diminishing from the hub to a small fraction of the maximum width, reducing this negative
376   effect. No claim is made that the estimates in Table 3 are accurate. Chord widths are confidential and
377   have been estimated from photographs. No account has been taken of the rate of twisting of the blades.
378   Such reduction in the pitch near the tip selectively reduces the back torque.

379
380   *Relationship of vortical entropic energy and Gibbs field to the governing equation of fluid motion*
381   The governing equations of fluid motion as formulated by Bernoulli, Laplace and others proposed no
382   such reversible heat-work process for vortices, except absorption and release of heat depending on
383   whether air is expanding or being compressed as in adiabatic processes. For streamlines as in a laminar
384   wind flow, the Bernoulli equation (12) relates kinetic energy ($\rho v^2/2$), the static pressure energy P
385   ($\Sigma mv^2/3=pV$) and gravitational potential energy, regarded overall in steady flow as constant.

386
387                          $$\rho v^2/2 + P + \rho gh = K \qquad (9)$$
388

12

389   The equation is also the basis of the theory that the pressure on the longer profile of an airfoil will be
390   lower, given that $\rho v^2/2 + P$ should be constant. The greater velocity required for air flow with a longer
391   path requires that the pressure P must fall, reducing the downward force. Despite widespread
392   acceptance of this theory, clear evidence for confirmation is difficult to find.

393

394   The vortical entropic energy first proposed in (Kennedy and Hodzic, 2021a) as $S_{vort}T$ must be added
395   to the total heat content indicated by the Clausius entropy of air (3,4), with the vortical component able
396   to be released in compressive or turbulent frictional processes. The same categories of energy
397   transformation are also observed in the Carnot cycle, varying during the isothermal and adiabatic
398   stages. We have extended this hypothesis (Kennedy and Hodzic, 2021b) to show how this internal
399   work that Clausius named the *ergal* amounts to a decrease in the Gibbs energy in equation (13). To
400   the extent that the vortical motion provides an additional degree of freedom for energy storage at a
401   larger scale, another term needs to be added to the Bernoulli equation.

402

403    $$\rho v^2/2 + P + \rho gh + S_{vort}T = K + Nk\tau ln[@_{vort}/\hbar] \qquad (10)$$

404

405   This can be thought of as a radial form of quantum state or potential energy, capable of being released
406   in defined meteorological conditions. We refer to this resonant energy field as the Gibbs field (-G) and
407   it comprises an addition to Clausius' ergal as a work process internal to the atmosphere.

408

2.4 Evidence of vortical heat produced by wind farms

410   In a previous paper (Kennedy et al., 2019) we showed that surface air heated from absolute zero to
411   298.15 K needs 2.4 MJ per cubic meter, including its kinetic energy. This implies that the vortical
412   energy of air in laminar flow at 1000 km of 15 meters per sec from the center of an active anticyclone
413   contains about 0.42% more wind-reversible field energy than at its non-rotating center. The data in
414   Tables 3 and 4 of possible heat capacities in the wind suggests an alternative explanation. This source
415   would be the release of latent heat in wind of vortical entropic energy, a result of turbulence caused by
416   turbines. The concept of vortical entropy was advanced by as a new class of potential risk to be
417   considered in climate change. The kinetic energy of wind of 10 m per sec is only 61 J per cubic meter.

418
419

420   **Table 4. Potential for heat release from turbulence caused by 1.5 MW wind turbines**

Turbulent process	Vortical energy J/m³	Heat released J/turbine/sec	Heat released wind farm 70 GE units J/sec	Volume air heated 3 ºC, m³ per sec	Height of warmer air moved 10 m/sec
Difference	13593.26	5.4370x10⁷	3.8059x10⁹	1.036x10⁶	103.6 m
20 declined to 10 m/sec		200 m² blades, 20 m/sec		C_p 1.225x10³/m³	1 km wide front

421
422

423   Should the laminar flow be impeded by surface roughness, causing turbulence, some of the vortical
424   energy will be released, warming the surroundings. For example, as detailed in Table 4, if wind speed
425   of 20 m per sec is effectively reduced by turbulence to a speed of 10 meters per sec, some 54 MW of
426   vortical turbulent heat is predicted to be released from air impacting the blades, heating the surrounding

13

427 molecules moving downwind. Given a heat capacity of 1.225 kJ per cubic meter for air, this is
428 sufficient to heat 6,122 cubic meters of air 1 degree Celsius. A windfarm 1 km wide generating 100
429 MW of power from 70 GE 1.5MW turbines is predicted to release 3800 MW of heat, moving 3.1
430 million cubic meters of air 10 meters downwind a second, raising air temperature 3 degrees Celsius in
431 a column about 100 m high. This prediction can readily be directly tested but is consistent with
432 published observations.

433

434 **2.5 *Environmental effects of heat production***
435 Given the prediction of significant heat production in section 5.1, the environmental effects of wind
436 farms should be of concern. In particular, their potential effect on evapotranspiration downwind as a
437 result of turbulence should be considered. Application of the Penman-Monteith equation is the usual
438 method to model evapotranspiration, including evaporation from soil or water surfaces as well as
439 transpiration of water used by plants to absorb nutrients, maintain plant turgor and provide water for
440 photosynthesis. Despite its importance for plant growth in the assimilation of carbon dioxide, the actual
441 consumption of water for plant growth is far less than that transpired. The inputs required are daily
442 mean temperature, wind speed, relative humidity and solar radiation. To assist investigation of causes
443 and effects for these events affecting bushfire risk, we are employing the Penman-Monteith equation
444 (*UFlorida* 2020 *AE459*), with data potentially of use from the MODIS satellite.

445

446 In equation (11) for evapotranspiration (*ET*), factors Rn and G indicate solar radiation and local
447 absorption of heat into the soil, ρ_a represents atmospheric density, C_p the heat capacity of air, e_s^o mean
448 saturated vapour pressure (kPa), r_{av} bulk surface aerodynamic resistance for water vapor, e_s mean daily
449 ambient vapor pressure (kPa) and r_s the canopy surface resistance (s m^{-1}).

450

451
$$ET_{sz} = \frac{[\Delta(Rn - G)] + [86,400\frac{\rho_a C_p}{r_{av}}(e_s^o - e^a)]}{(\Delta + \gamma(1 + \frac{r_s}{r_{av}}))}$$
(11)

452

453 Wind speed *u* is also included in the numerator. The main drivers of evapotranspiration are heat from
454 solar radiation, plant growth, environmental conditions of temperature and relative humidity as well
455 transport away in air. More important than wind speed, turbulence has now been shown to significantly
456 increase evaporation, as eddy diffusion lengthens the trajectory for water vapor molecules. Since
457 terrestrial wind farms are usually placed in rural areas, we are applying this model to test our prediction
458 that they may contribute to dehydration of the landscape downwind from turbines, increasing fire risk.
459 We will discuss how these proposals may be tested experimentally, including by observations from
460 the MODIS satellite.

461

462 To determine the potential effects of wind turbines on evapotranspiration, we calculated
463 evapotranspiration at a range of windspeeds, and then recalculated it with a 1 degree C increase in
464 temperature assumed to be the result of wind turbines (Table 6). A 1 degree increase in temperature
465 was used as we found from that turbulence caused in the wind at 20 m per sec by wind turbine blades
466 effectively reducing laminar speed to 10 m per sec which could release enough heat to raise the
467 temperature downwind in a swath of 100 m wide and 250 m high more than 50 km downwind by 1

14

468 degree Celsius. We used the Penman-Monteith equation for the 5th February at -30.39 latitude, 275 m
469 elevation and assumed effective daylength of 9.25 hours.
470

471 **Table 5.** Predictions regarding heat production and evapotranspiration for 1 °C on wind farms

Wind speed (m sec^{-1})	Evapotranspiration (no wind farm)	Evapotranspiration (with wind farm)	Delta ET (mm day^{-1})
5.0	7.31 mm day-1	7.52	0.21
10.0	10.18	10.52	0.34
15.0	12.02	12.46	0.44
20.0	13.30	13.82	0.52
25.0	14.24	14.82	0.58

472
473

474 The FAO version of the Penman-Monteith equation was applied using the python module ETo, and
475 only the values described here were altered. For both temperature and relative humidity, minimum
476 and maximum values were 20 and 30 C, and 25 and 84%. Evapotranspiration rates calculated without
477 heat input from turbulence induced by the wind turbines are compared with rates corrected with a 1
478 degree increase in minimum and maximum temperatures, with all else unchanged. The
479 evapotranspiration is between 0.21 mm/day at 5 m/s to 0.58 mm/day at 25 m/s. These predictions, and
480 the short- and long-term effects on the dryness of soil and plants, need to be tested experimentally.
481 Clearly, at elevated wind speeds over multiple consecutive warm to hot days, the additional quantity
482 of moisture removed from the soil and vegetation due to wind turbines has the potential to be
483 substantial. Our calculation in Table 6 has taken no account of the downwind turbulence that may
484 increase evapotranspiration significantly (Cleugh, 1998; Navaz et al., 2008).
485

486 If these results are found in rural landscapes where wind farms are located, they would indicate
487 increased risk with respect to optimum agricultural or pastoral productivity. However, in some cases
488 increased temperature and reduced water-holding capacity of air may be beneficial for plant growth,
489 particularly in environments with ample water supplies. By contrast, in drought prone conditions like
490 most of Australia, negative effects on productivity and increased fire risk can be assumed. There is a
491 need for these factors to be assessed wherever wind farms are developed.
492
493

494 3. **Discussion**
495

496 The radial action model for wind turbines resulted from the search for an imaginative hypothesis that
497 could be tested, on the lines recommended by the late Karl Popper. The initial computer program
498 described in Methods was used to develop the model by a reiterative process of trial and error.
499 Equations (4) and (5) became available only after this process was complete when results and
500 experience with real wind turbines were found in agreement. It is doubtful if this result could have
501 been achieved with a higher-level computer language. These equations now form the basis for
502 presenting the model in other computer codes, like Mathematica and Python available in
503 Supplementary Text.
504

15

505 The calculation of wind power to the cube of wind speed shown in Equations 1 and 2 considers the
506 rate at which kinetic energy of air flows through the circular profile area traced by the tips of the
507 rotors. However, only a fraction of this air can be intercepted by the blades, despite appeal to
508 concepts like solidity with respect to the air. Particularly in the larger modern turbines most of the air
509 flow must pass through unimpeded, given that the blades normally represent only some 3-4% of the
510 area of the rotor circle. Thus, it is likely that no more than 5% of the air volume is initially made
511 turbulent, effectively tracing triplicate rotary spirals of turbulent air downwind, balancing the work
512 done on the turbine rotors for transmission into the dynamo.
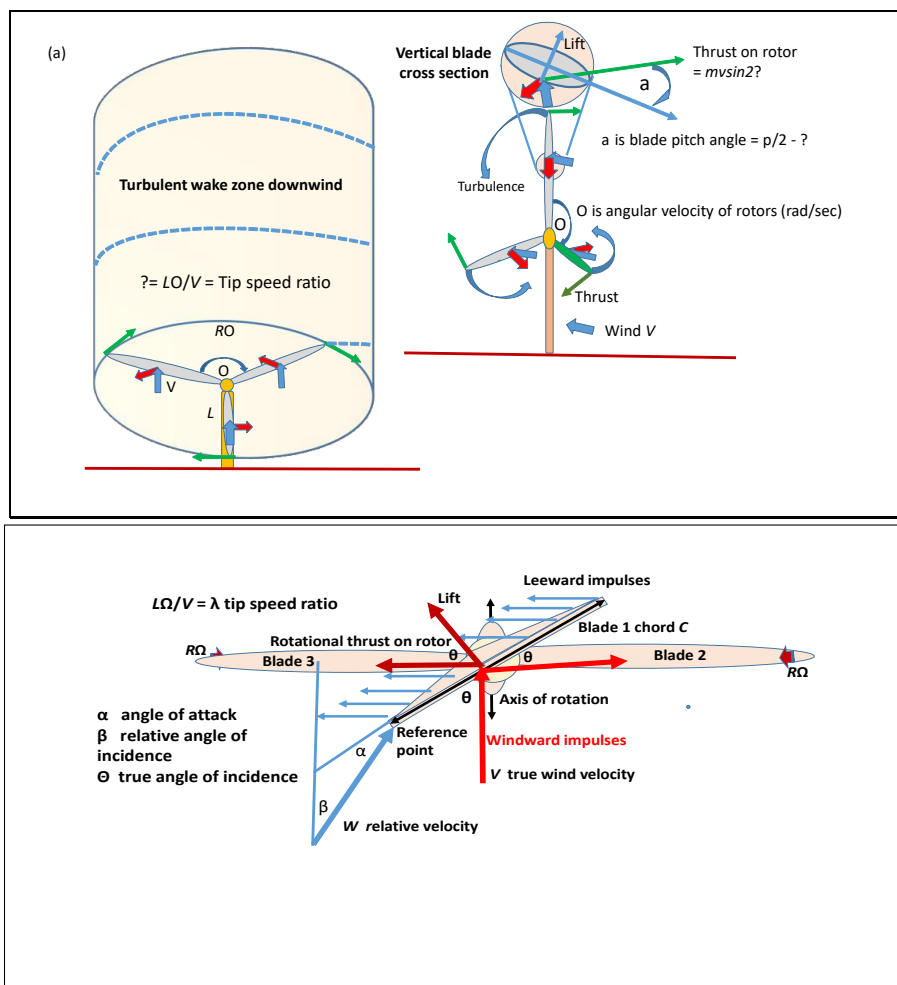
513

514 The leeward torque absent from BEM theory performs work normal to the air flowing into the cavity
515 behind the blade, up to about 25% of the power generated (Table 1). Additional release of radiant heat
516 by turbulence is predicted to be a feature of the operation of wind turbines, possibly more than five
517 times power generation if the vortical energy hypothesis is confirmed. We hypothesize a significant
518 warming effect downwind that may also increase evaporation, caused by temperature increase and
519 turbulent surface interaction with vegetation and soil surfaces. This prediction should be tested for
520 quantification, to be included in productivity models or estimates of fire risk, as a matter of due
521 diligence.

522

3.1 *Reconciliation of radial action and blade element momentum models*

524 The theoretical success of this model calls for some comparison with the blade element momentum
525 (BEM) model based on airfoil and Bernoulli fluid motion equations. In Figure 5(a) aspects of the two
526 different approaches are given on one diagram, highlighting some differences. The radial approach we
527 introduce involves two classes of action, quantifying inertial impulses of momentum at each radius of
528 the rotor blade surfaces, one windward and the other leeward. In the figure, the pitched blades are
529 regarded as rotating normally to the true wind direction with the turbines facing the wind turning
530 anticlockwise. Air in inertial motion between the rotors is unimpeded with the blades reflecting
531 windward impulses at the true angle of incidence (θ). Only a small proportion of the air stream will
532 impact the blades depending on the proportional area of the circle with radius L. If stationary,
533 obstruction by the blade must create a region of low pressure to its rear. Once a steady state of rotation
534 Ω is reached, the blade still obstructs air flow as before but its rear surface impacts resisting air normal
535 to the blade's motion, deflecting it with the action impulses a function of the radial speed of rotation
536 ($R\Omega$). For most of the blade except near the hub, the pressure at the rear of the rotating blade must be
537 increased above that in the wind. However, there is no diminution of pressure exerted on the windward
538 surface because fresh air continually occupies this space. Except near the hub, air at the rear of the
539 blade is strongly compressed so that no drag in the same direction as the wind is possible, turbulence
540 caused by diminished pressure.

541

16

542

543
544 **Figure 5. (a)** Plan and elevation of wind turbine showing clockwise motion with parallel pitching of all three
545 blades ($\pi/2 - \theta$) to the plane of rotation with rotor thrust normal to the wind stream. For a tip speed ratio (λ)
546 equal to 12 for wind velocity (V) of 10 m/sec, the rotor tips travel 120 meters while the wind advances 10 meters.
547 Lower: Comparison of blade element momentum (BEM) and radial action theory (RA). BEM subsumes the
548 reverse or back torque (T_B) as an effect giving relative wind velocity (W). T_w is derived by integrating the
549 windward action impulses along the blade to the hub and T_B integrates the backward push action impulses
550 exerted by the blade.
551
552

553 The windward impact pressure is independent of the radius unless the blade is pitched with length,
554 varying by sin θ, affecting the volume of air impacting the blades per sec. While the intensity of
555 impulses is constant for a blade surface with a constant pitch, the rate of action or torque varies with
556 radius, requiring integration for the turbine. By contrast, the impulses produced by the leeward surface
557 of the blades vary with the radius squared, once for the surface area of air impacted normal to the
558 rotation per sec and once more for the radial variation in momentum As action impulses.
559

17

560 We have no intention to describe BEM theory (Schubel and Crossley, 2012) in detail. However, in
561 using a Bernoulli approach to airfoil theory BEM considers lift normal to the blade and drag directed
562 horizontally along the surface in the wind direction as the two main forces operating. To determine
563 relative wind velocity the variable speed of an observation point on the rotating blade is taken. If near
564 the hub, there is little change of direction (θ- β) but near the tip, the apparent angle of incidence
565 diminishes. In Figure 5(a), the pitch angle to the chord line of the blade is 90-θ degrees, becoming zero
566 when the true wind is normal to the blade, with no power to cause rotation. Alternatively, the pitch
567 may be increased to 90º, when the back torque, while the blade is still spinning, will exceed the almost
568 zero windward torque. Many of the performance studies on horizontal turbines have been performed
569 with 'frozen' rotors (9), experiments conducted with variable speeds in wind tunnels enabling
570 theoretical power to be calculated. However, BEM avoids consideration of back torque that impedes
571 rotation.

572

573 Figure 5(b) shows a simulated wind turbine with 40 meter blades similar to the General Electric
574 (GE1.5) model, generating an average of some 1.5MW of power while rotating clockwise. Note that
575 by contrast, Figures 1 and 2 would produce a counter-clockwise rotation observed from the windward
576 direction. The blades represent about 3-4% of the area swept. While most of the air in the wind can
577 pass between the blades unimpeded, some 10% of the air flow could be subjected to turbulent
578 conditions. This suggests there is no requirement for a significant decrease in downstream windspeed,
579 as is required using the BEM kinetic energy model because of the significant decrease in kinetic energy
580 required. We argued in Section 5 that a lateral source of vortical potential energy sustains the kinetic
581 energy, except in the turbulent volume where thermal energy will be released. This prediction of radial
582 action mechanics can readily be tested.

583

584 We emphasize that the main purpose of this article is to develop a testable hypothesis explaining the
585 maximum power in an ideal wind turbine, assuming the output is linked reversibly to a work process
586 such as electricity generation. This purpose is similar to Sadi Carnot's proposal that the main purpose
587 of his heat engine cycle was to describe the most efficient cycle. However, the environmental effect of
588 turbulence must be examined as it is a key consequence of the radial action hypothesis.

589

590 **3.2 *Wind turbine blade design, twist and other modulations in rotors***
591 The BEM theory justifies the twisting of the blade, reducing the pitch towards zero degrees
592 approaching the tip (Schubel and Crossley, 2012). A twist is also justified in radial action diminishing
593 the back torque proportional to R^2 nearer the tip whereas the windward torque is no more per *unit* area
594 nearer the hub. This property could easily be introduced into the radial action model by varying the
595 relative angle of inclination towards the tip. Further airfoil refinements commonly engineered into the
596 rotors can easily be incorporated. These are considered to minimize frictional effects on turbines,
597 making an independent contribution to the efficiency of power output. Incorporating design features
598 that are responsive to wind speed and other factors may optimize this process, which can be confirmed
599 empirically.

600

601 This new understanding of power generation from radial action theory accepts the value of research
602 on optimizing blade design. Factors such as variation in thickness and twist of the chord pitch will still
603 provide advantages in power output if correctly analyzed. Schubel and Crossley (2012) have provided

604 a detailed review of the current state of the art of blade design, highlighting efficiency to be gained
605 from design principles based on blade shape, airfoil properties, optimal attack angles using relative
606 wind speed and gravitational and inertial properties. With suitable corrections offered by the radial
607 action approach to wind force, lift and thrust factors and generation of action most of this theory can
608 be remodeled quite easily.
609
610 The Betz limit is considered to exert an effect on BEM theory but has no place in radial action
611 mechanics. Only a small proportion of the available vortical energy is consumed, but a different kind
612 of limit emerges in the competition between windward and leeward torques, with the latter becoming
613 more significant as the length of turbine blades increases.
614

615 ### 3.3 *Heat production from turbulence*
616 In developing turbulence, the largest scale eddies nearer laminar flow are regarded as containing most
617 of the kinetic energy, whereas smaller eddies are responsible for the viscous dissipation of turbulence
618 kinetic energy. Kolmogorov described by Frisch (1995) hypothesized that the intermediate range of
619 length scales could be statistically isotropic, and that a temporary form of equilibrium would depend
620 on the rate at which kinetic energy is dissipated at the smaller scales. Dissipation is regarded as
621 the frictional conversion of mechanical energy to thermal energy, effectively radiation, raising
622 temperature. In vortical action theory, the kinetic energy is regarded as always complemented by the
623 Gibbs field vortical energy and the dissipation process loses kinetic energy, a result and coincident
624 with the loss of the field energy. The dissipation rate may be written down in terms of the
625 fluctuating rates of strain in the turbulent flow and the fluid's kinematic viscosity, v, that has
626 dimensions of action per unit mass. We suggest that the failure to obtain analytical solutions for
627 turbulent processes may solved if these complementary forms of energy are considered.
628
629 Current practice for wind power makes no provision for heat production other than minimizing friction.
630 The radial action theory demonstrates that the back torque exerted by turbines is effectively a work-
631 heat dissipation of wind energy, contributing to its evolution locally at the point of power output.
632 Depending on the factors controlling efficiency, this heat production can be considered as less but of
633 the same order as the power take-off as electrical energy.
634
635 Of more concern could be additional heat release downwind from turbulence. In Table 4, we provided
636 estimates, showing that turbulent release is significantly greater in magnitude. While direct heat
637 production at the turbine is not expected to make a significant difference to air temperature, together
638 with turbulence, a significant fall in the relative humidity of air passing over vegetation and soil
639 together with greater surface interaction by turbulent air can be anticipated. The vortical degree of
640 freedom of motion or action is characterized by its large radius of action, effectively storing latent heat
641 that can be released as radiation in turbulent conditions. It is known that the kinetic energy in laminar
642 flow is not retained in the turbulent motion of air or water moving on much shorter radii of declining
643 scales. Radial action theory predicts this will be the case, the loss of kinetic energy expected as
644 potential energy we have referred to as Clausius' *ergal* (5) or internal work is released. The kinetic
645 motion in the system at all scales is sustained by such field or quantum state energy. This is a
646 consequence of the virial theorem, also explained by Clausius.
647

WIND
ENERGY
SCIENCE
DISCUSSIONS
european academy of wind energy

19

648   The impacts of wind farms on surface air temperatures are well documented. Roy and Traiteur (2012)
649   claimed that this regional warming of almost 1 ºC compared to an adjacent region resulted from
650   enhanced vertical mixing from turbulence generated by wind turbine rotors. Warmer air from above
651   the surface, particularly at night, was claimed to be forced to the surface. Harris et al. (2014) showed
652   "irrefutable night-time warming relative to surrounding areas using observations made from eleven
653   years of MODIS satellite data with pixel size of 1.1 km^2. The same conclusion was reached by Miller
654   and Keith (2018), showing a significant night-time warming effect at 28 operational US wind farms.
655   They also concluded that wind's warming could exceed avoided warming from reduced carbon
656   emissions for more than a century. According to Miller (2020) these effects on warming are detectable
657   tens of kilometers downwind.
658
659   However, the opinion that the warming is a result of overturning temperature inverted air at night is
660   not convincing. This conclusion is apparently based on an argument that this was the only source of
661   warmer air considered as available. Vortical heat release now obviates such reasoning. More direct
662   observations using instruments sensing simultaneously, both upstream and downstream of wind farms,
663   is required to establish the source of warming, particularly in higher daytime temperatures.
664
665   **3.4 *Independent evidence of vortical potential energy as a heat source released by turbulence***
666   Chakirov and Vagapov (2011) describe a method for direct conversion of wind energy into heat using
667   a Joule machine. They show that turbulence in a rotating fluid with Reynold's number (*R*e) greater
668   than 100,000 provides warmth not obtained when the flow is laminar. By insertion of baffles to cause
669   turbulence in the flow path of water set in rotation in a smooth cylinder using direct wind power, they
670   demonstrate that needs for room heating in polar regions can be satisfied. It is well known that the
671   kinetic energy in turbulence is not conserved at lower fractal scales, suggesting that any entropic
672   energy or ergal is also lost in these processes, where work performed is dissipated as heat by friction.
673   We have recently discussed such heat-work-heat cycles in an action revision of the Carnot Cycle,
674   emphasizing the importance of entropic field energy as the negative of the Gibbs energy. The
675   molecular kinetic energy in such systems is a small fraction of the total non-sensible heat, stored in
676   quantum state activations of translation, rotation and vibration.
677
678   Chervenkov et al. (2013) have shown how the kinetic energy and temperature of polar molecules can
679   be reduced with a centrifugal force from around 100 K to 1 K, A redistribution of field entropic
680   potential energy from interior molecules that can be retrieved nearer the center of the centrifuge is
681   regarded as the cause of the cooling. Geyko and Fisch (2013, 2016) reported measuring reduced
682   compressibility in a spinning gas where thermal energy is stored in their theory of the piezo-thermal
683   effect . This extra heat capacity at constant temperature indicates an additional degree of freedom, that
684   we conclude is vortical, supplementing the well-recognized vibrational, rotational and translational
685   action as degrees of thermodynamic freedom (3-5).
686
687   The widespread failure to recognize the dominance of this nonsensible field energy as real potential
688   energy (actually, kinetic energy of quanta at light speed [$T = mc^2$, J]) in natural systems, favoring the
689   sensible kinetic heat indicating the temperature of molecules, has been a critical omission as we
690   showed in our estimation of the entropy of atmospheric gases and revision of the Carnot cycle. In
691   effect, potential energy in the atmosphere can be gravitational varying vertically, but it can also be

stored horizontally as vortical energy. These two forms of energy, kinetic and entropic as negative Gibbs energy, are complementary in operation and one must always have one to have the other. With viscous dissipation of energy in storms it is not just the turbulent kinetic energy that is released in a turbulent cascade (Businger and Businger, 2001), but also the vortical entropic energy much larger in magnitude that sustains the kinetic energy. Of course, it is the current enthalpy sustained by the Gibbs field that actually does the physical damage, as we confirmed for work performed in the Carnot cycle (Kennedy and Hodzic, 2021a).

By coupling a Newtonian approach regarding momentum transfer to radial action mechanics (20) regarding torques generated by rates of action impulses as in Gibbs fields we claim we have provided an effective method to estimate maximum power extraction from wind turbines. We claim the following advantages for the new theory, all subject to experimental refutation or confirmation.

- A more effective mathematical model of wind power output. Using the Carnot approach for power of heat engines, the radial action method allows maximum power to be estimated.
- A better template for wind turbine design is also provided, giving an expected closer correspondence between theoretical and practical results.
- A means of optimization of wind power and to minimize heat output is now available. This has the potential to be applied as control theory for managing turbines, either solitary or in wind farms. It is noteworthy that the action mechanics theory developed in this theoretical study suggests that only a small proportion of the potential power of wind in laminar flow is utilized, unlike the BEM theory based on harvesting kinetic energy.
- Environmental protection is also a possible output from using the action model. Ways to manage turbulence to reduce its possible negative effects can be topics for research, seeking to avoid unintended environmental consequences of this burgeoning technology as a prime source of renewable energy.

We emphasize that this paper seeks to present hypotheses that still need rigorous testing. However, for science to advance it is essential that such hypotheses receive due consideration that only prominent publication will allow. This is even more important in an area critical to climate science and the management of climate. The potential of action mechanics to contribute to the science of ecosystems was advanced in 2001 (Kennedy, 2001). A preprint of the paper is also available on the arXiv site (Kennedy et al., 2021.

4. Methods

Results reported in the figures and tables are all calculated by exact computation under stated physical conditions and not subject to experimental variation.

4.1 *Wind turbine characteristics*

To allow testing of the radial action model for estimation of power outputs, approximate simulations of existing wind turbines were conducted using dimensions shown in Table 1. Blade lengths are advertised, but the maximum chords were estimates made from photographs. No account was taken of pitch values or twisting of the blade.

WIND ENERGY SCIENCE DISCUSSIONS
eawe european academy of wind energy
Open Access

21

4.2. *Computer Model*

Equations (4) and (5) were determined as results by careful attention to physical dimensions (ML^2/T^2), confirmed by the variations in the torques observed in the numerical model, rather than from calculus or basic theory. A key specification was that the radial action wind turbine model should give good results for wide variations in the power outputs predicted, varying with rotor length and blade area from watts to megawatts.

The numerical computer program given in Supplementary Text employed inputs including wind speed (v), angle of wind incidence (θ) and tip-speed relative to wind speed, defining a managed angular velocity [Ω, radians sec^{-1}] for the turbines. The program was also designed to allow learning by experience. The complexity of current BEM models suggested that a simpler means to determine wind power based on Newtonian physical principles was needed. Our recent papers (3-5) on action mechanics provided physical background to this work.

Elucidation of the governing equations was a result of analyses using numerical methods. The program focused on the calculation of the rate of action impulses [$\delta mvR/\delta t$] as torques, also calculating swept area throughput of concurrent kinetic energy for comparison. Generated on a Windows 10 platform with a capable Texas Instruments SR52 TRS32 emulator, the program is available as Supplementary Text has also been prepared using Mathematica with a Notebook suitable for blades with constant chord C is also available.

To render the program in other systems such as Python and Mathematica, equations (4) and (5) for windward and leeward torques were coded only for relevant sections of the program, without estimates of kinetic energy in swept areas.

References

Businger, S., and Businger, J. A.:Viscous dissipation of turbulence kinetic energy, J. Atmos. Sci., 58, 3793-3796, 2001.

Chakirov, R., and Vagapov, Y.:Direct conversion of wind energy into heat using Joule machine, Int. Conf. Environ. Comp. Sci. **19**, 12-17, 2011.

Chervenkov, S., Wu, X., Bayerl, J., Rohlfes, A. Gantner, T., Zeppenfield A., and Rempe, M. G.:Continuous centrifuge decelerator for polar molecules. arXiv:1311.7119v1 (2013).

Cleugh, H. A. Effects of windbreaks on airflow, microclimates and crop yields. Agrofor. Sys. 41, 55-84, 1998.

Frisch, G. Turbulence: The legacy of A.N. Kolmogorov, Cambridge University Press, 1995.

22

780 Geyko, V. I., and Fisch, N. J.:Reduced compressibility and an inverse problem for a spinning gas.
781 Phys. Rev. Lett. 110, 150604, 2013.
782
783 Geyko, V. I., and Fisch, N. J.:Piezothermal effect in a spinning gas. Phys. Rev. *E*94, 042113, 2016**.**
784
785 Glauert, H., Airplane propellers. In Aerodynamic Theory. Springer Berlin/Heidelberg Germany,1935.
786
787 Gupta, S., and Leishman, J. G.:Dynamic stall modelling of the S809 aerofoil and comparison with
788 experiments. Wind Energy 9, 521-547, 2006.
789
790 Harris, R. A., Zhou, L., and Xia, G.:Satellite observations of wind farm impacts on nocturnal land
791 surface temperature in Iowa. Remote Sens. 6, 12234-12246, 2014.
792
793 Kennedy, I. R.:Action in Ecosystems: Biothermodyamics for Sustainability. Research Studies
794 Press/John Wiley Baldock, UK, 251 p., 2001.
795
796 Kennedy, I. R., Geering, H., Rose, M. and Crossan, A.:A simple method to estimate entropy and free
797 energy of atmospheric gases from their action. Entropy, 21,454-470, 2019.
798
799 Kennedy, I. R., and Hodzic, M.:Action and entropy in heat engines: An action revision of the Carnot
800 Cycle. Entropy 23, 860-887, https://doi.org//10.3390/e23070860, 2021.
801
802 Kennedy, I. R., and Hodzic, M.:Partitioning entropy with action mechanics: Predicting chemical
803 reaction rates and gaseous equilibria of reactions of hydrogen from molecular properties. Entropy 23,
804 1064-1086, 2021,
805
806 Kennedy, I. R., Hodzic, M., Crossan, A.N., Acharige, N. and Runcie, J.:A new theory for estimating
807 maximum power from wind turbines: A fundamental Newtonian approach. arXiv preprint
808 arXiv:2110.15117.
809
810 Miller, L. M. , and Keith, D. W.:Climatic impacts of wind power. Joule, 2, 2618-2632, 2018.
811
812 Miller, L.:The warmth of wind power. Physics Today, 73, 58-63, 2020.
813
814 Navaz, H.K. , Chan, E., and Markicevic, B.: Convective evaporation model of sessible droplets in a
815 turbulent flow – comparison with wind tunnel data. Mech. Eng. Publ., 149, 2008.
816
817 Roy, S. B. , and Traiteur, J. J.:Impacts of wind farms on surface air temperatures. PNAS, 107, 17899-
818 17904, 2012.
819
820 Schubel, P. J., and Crossley, R.J.:Wind turbine blade design. Energies, 5, 3425-3449.
821 doi:10.3390/en5093425, 2012.
822

23

823 Sorensen, J. N.:General Momentum Theory for Horizontal Axis Wind Turbines. Springer, Cham
824 Switzerland, 2015.
825
826
827
828
829